PERGAMON
International Journal of Heat and Mass Transfer 41 (1998) 2877–2892
International Journal of HEAT and MASS TRANSFER

A simplified wide band model of the cumulative distribution function for water vapor

O. Marin, R. O. Buckius*

Department of Mechanical and Industrial Engineering, University of Illinois at Urbana-Champaign, 1206 West Green Street, Urbana, IL 61801, U.S.A.

Received 1 July 1997; in final form 5 January 1998

Abstract

A simple and accurate model to describe the wide band absorption coefficient cumulative distribution function is developed. The model, based on exact limiting formulations of the cumulative distribution function, explicitly expresses the absorption coefficient in terms of the cumulative distribution function, simplifying the solution of the radiative transfer equation. Parameters for the 1.38, 1.87, 2.7 and 6.3 μm bands of water vapor are developed for a wide range of pressures and temperatures from 300 to 2900 K. The parameters for the rotational band of water vapor include temperatures from 300 to 1900 K. The results obtained with this simplified model are in good agreement with existing narrow band and line-by-line results. The simplified cumulative distribution function model provides a wide band absorption consistent with alternate methods. © 1998 Elsevier Science Ltd. All rights reserved.

Nomenclature

A	wide band absorption [cm^{-1}]
A^*	nondimensional wide band absorption
b	line halfwidth [cm^{-1}]
b_B	self-broadening to foreign-gas broadening ratio
B	pressure broadening parameter, $B = b/d$
C	coefficient in exponential wide band formulation
d	line spacing [cm^{-1}]
e	2.7182818...
f	distribution function
g	cumulative distribution function
k	absorption coefficient [m^2 g^{-1}]
L	layer thickness [m]
n	empirical factor for P_e
N	number of elements in summation
P	pressure [atm]
P_e	effective pressure [atm]
R	ratio, $R = s_{max}/s_{min}$
s	line intensity divided by line spacing [m^2 g^{-1}]
s_{min}	minimum line intensity [m^2 g^{-1}]
s_{max}	maximum line intensity [m^2 g^{-1}]
S	line intensity [cm^{-1} g^{-1} m^2]
T	temperature [K]
u	mass pathlength [g m^{-2}]
w	weight factor for Gaussian integration
W	fitting function
x	variable.

Greek symbols

α	integrated band intensity [cm^{-1} g^{-1} m^2]
β	broadening parameter
δ	difference
$\Delta\nu$	wavenumber interval [cm^{-1}]
κ	nondimensional absorption coefficient
ν	wavenumber [cm^{-1}]
ρ	density [g m^{-3}]
ω	bandwidth parameter [cm^{-1}].

Subscripts

0	band center or band head, reference band parameters
A	wide band absorption
B	subscript in self-broadening to foreign-gas broadening ratio
$B \to 0$	small pressure broadening parameter limit
$B \to \infty$	large pressure broadening parameter limit
c	complete model described by equations (10)
e	exact
i	summation parameter

---

* Corresponding author.

0017-9310/98 $19.00
PII: S0017-9310(98)00033-7

k	absorption coefficient
l	lower
Lorentz	Lorentz absorption line
m	model
max	maximum
min	minimum
nb	narrow band
q	quadrature
u	upper
wb	wide band.

1. Introduction

The gas absorption coefficient is the fundamental property in the solution of the radiative transfer equation. Problems involving gray absorption and emission properties, where the absorption coefficient is constant over a certain spectral interval, are more easily solvable than nongray problems. Real gases are nongray and the absorption coefficient varies substantially over narrow spectral intervals. The integration of the equation of transfer requires detailed information on the gas spectral radiative characteristics. Several methods to evaluate the absorption coefficient or the gas absorption have been developed. Each of the methods accounts for the gas radiative properties within a certain spectral interval. The magnitude of this spectral interval defines the type of the method used, as well as the accuracy and the computational effort. The line-by-line method is the exact approach of calculating the local absorption coefficient, directly from the rotational–vibrational line structure. The effects of each participating line at a certain spectral location are summed, providing the magnitude of the spectral absorption coefficient. Since within a rotational and vibrational band there are thousands of absorption lines, the computational effort required to calculate the spectral absorption coefficient is substantial. Line-by-line calculations for thermal transport applications that require analysis of the entire spectrum must access very large databases containing the spectral information [1, 2].

Figure 1 shows the variation of pure water vapor absorption coefficient over the infrared spectral domain, obtained with the line-by-line method, for a water vapor pressure of 1 atm. The HITRAN database [1, 2] is used for the ambient temperature results (Fig. 1(a)) and the newly released HITEMP database [2] is used for 1000 and 1500 K, as presented in Figs. 1(b) and 1(c), respectively. Although the absorption coefficients presented in Fig. 1 are averaged over spectral intervals of 5 cm^{-1}, large variations of the absorption coefficient over relatively narrow spectral intervals can be observed. The spectral domains where the absorption coefficient is relatively large are termed as wide bands, and they occur due to molecular rotational–vibrational transitions. The highly nonuniform distribution of the absorption coefficient leads to computationally expensive solutions of the radiative transfer equation. In order to reduce the computational burden of the radiative transfer equation, several models that approximate the absorption characteristics of the gas over different spectral intervals have been developed. Commonly used models are the narrow band models [3, 4] generally valid for intervals of tens of cm^{-1}, wide band models approximating entire rotational–vibrational bands and total spectrum approximations.

The absorption coefficient distribution functions (*k*-distribution) over a specified spectral interval can be used to accurately solve transport problems in highly nonhomogeneous media [5, 6] and in the presence of scattering particles [7]. At the present time there is no simple, fundamentally-justified expression for the absorption coefficient cumulative distribution function over large spectral intervals. Marin and Buckius [7] use limiting forms to provide a quasi-empirical, complex expression for the absorption coefficient cumulative distribution function based upon the exponential wide band model applied to the Malkmus narrow band model [8]. Since the radiative transfer equation requires the explicit values of the absorption coefficient, the numerical inversion of the derived expression is required with an increased computational burden. Domoto [9] shows that the absorption coefficient distribution functions can be determined from an inverse Laplace transform of the transmissivity function and derives such expressions for several narrow band models. Lee et al. [10] and Parthasarathy et al. [11] use the same concept to derive reordered expressions of the absorption coefficient for wide band spectral intervals. The wide band cumulative distribution functions and the reordered absorption coefficient functions use the band parameters originally developed for the wide band absorption to estimate the absorption coefficient distribution function, introducing further approximations and sources of inaccuracies in the absorption coefficient distribution.

The limitations in the existing methods indicate the need for the development of a simple yet accurate, fundamentally justified methodology to determine the absorption coefficient distribution for a wide band spectral interval. Band parameters resulting directly from the absorption coefficient distribution function are necessary for improved accuracy. Marin and Buckius [12] develop limiting expressions for the absorption coefficient cumulative distribution function. This formulation is shown to accurately describe the general characteristics of the most dominant water vapor and carbon dioxide bands, for both small and large pressure limits. Marin and Buckius [12] show that the distribution function depends on the superposition of the participating rotational–vibrational bands for wide spectral intervals. The wide spectral intervals are classified into single wide bands and the resulting

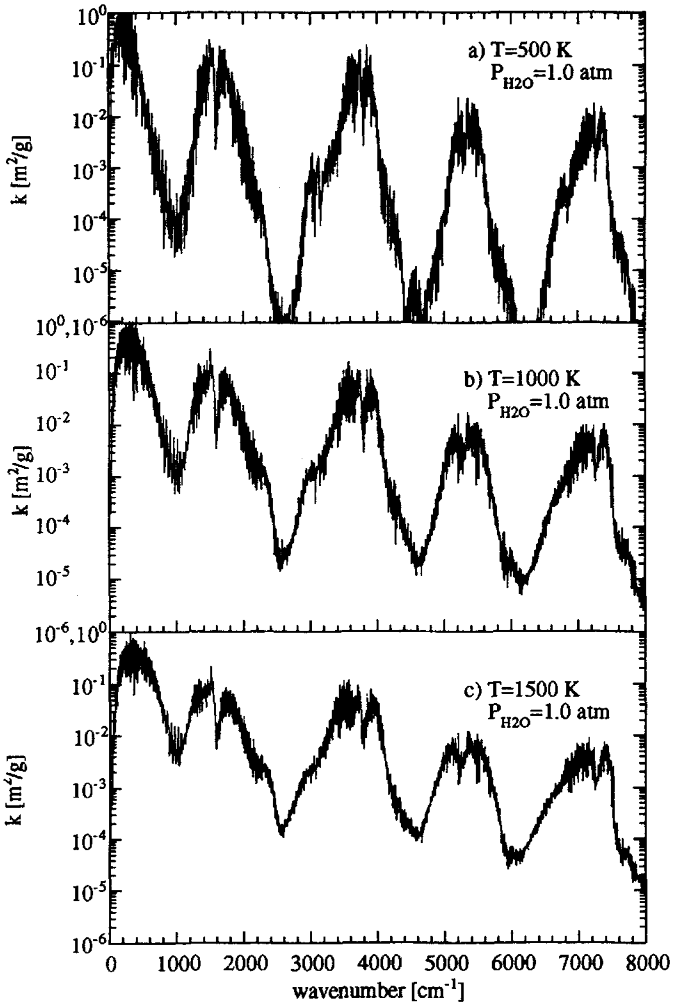

Fig. 1. Absorption coefficient variation for pure water vapor with a pressure of 1 atm over the infrared spectrum, with a spectral resolution equal to 5 cm^{-1}. (a) $T = 500$ K, (b) $T = 1000$ K and (c) $T = 1500$ K.

model must incorporate the dominant transitions that share the same spectral interval. It is concluded [12] that the water vapor bands can be modeled with the single dominant transition within each spectral interval. This formulation, together with additional physically-justified approximations, is used here for the development of a model for the absorption coefficient distribution function for wide spectral intervals. Since the original wide band parameters as described by Edwards [13–17] are designed to optimize the wide band absorption, it is expected that different parameters can better approximate the absorption coefficient distribution function. Band parameters for the five important bands of water vapor are developed for temperatures up to 2900 K (1900 K for the rotational band) and a wide range of pressures. The results are compared to both the exact line-by-line calculations [1, 2] and the narrow band results [3, 4]. The band absorption and emission produced by the simplified model are compared with existing models.

2. Exponential wide band $g(k)$ model

2.1. Pressure limits

This work attempts to model the absorption coefficient distribution function over large spectral intervals, including entire vibrational–rotational bands. In the small pressure limit it is assumed that the spectral interval consists of individual lines with different intensities and the same pressure broadcasting parameter. The line intensity variation within a wide band is assumed to be given by the Edwards band model [13–17]. According to this model, the line intensity-to-spacing ratio is maximum at the band center or band head, and it decreases exponentially towards the band wings.

In the small pressure limit, a narrow spectral interval is assumed to be populated by one single line since the interactions between neighboring lines may be neglected. Plass [18] shows that the narrow band absorption characteristics are dependent primarily on the average line intensity, while the line intensity distribution of the participating lines is of limited importance. The cumulative distribution function of the single line model, in the small pressure limit is approximated as [12]

$$g_{B\to 0,\mathrm{Lorentz}}(k) = 1-\sqrt{\frac{sB}{k}} \tag{1}$$

where k is the absorption coefficient, $B = b/d$ is the pressure broadening parameter, described as a ratio between the line halfwidth b and the line spacing d, and $s = S/d$ is the ratio between the line intensity S and the line spacing.

Equation (1) is used together with the exponential wide band model [13–17] to calculate the cumulative distribution function of the absorption coefficient for the entire wide band [12] as

$$g_{B\to 0,\mathrm{wb}}(k) = \frac{1}{\ln(R)}\int_{s_{\min}B}^{\min(k,s_{\max}B)} \frac{1}{x}\left(1-\sqrt{\frac{x}{k}}\right)\mathrm{d}x \tag{2}$$

where $s_{\min}$ is the minimum line intensity-to-spacing ratio in the wide band, and $R = s_{\max}/s_{\min}$ represents the ratio between the maximum and the minimum line intensity-to-spacing ratios, which can also be expressed as $R = \exp(\Delta\nu/\omega)$, where $\Delta\nu$ is the spectral interval of the band and ω is the bandwidth parameter. The maximum line intensity-to-spacing ratio is calculated as $s_{\max} = \alpha/\omega$, where α is the integrated band intensity. The inverse function in the integral results from the exponential band model line intensity distribution function [12]. Equation (2) can be integrated to yield a closed form solution for $g(k)$ as

$$g_{B\to 0,\mathrm{wb}}(k) = \begin{cases} 0 & \text{for } k < s_{\min}B \\ \dfrac{1}{\ln(R)}\left[\ln\left(\dfrac{k}{s_{\min}B}\right)-2+2\sqrt{\dfrac{s_{\min}B}{k}}\right] & \text{for } s_{\min}B \leqslant k \leqslant s_{\max}B \\ 1-\dfrac{2}{\ln(R)}(\sqrt{R}-1)\sqrt{\dfrac{s_{\min}B}{k}} & \text{for } k > s_{\max}B \end{cases} \tag{3a,b,c}$$

The expressions in equations (3) accurately describe the wide band model for small values of the pressure broadening parameter. The cumulative distribution function expressed by equations (3) is in good agreement with existing models in this limit [7]. A limitation of the formulation in equation (3b) is that it cannot be inverted analytically to yield an expression for the absorption coefficient. It is noted that the exponential band model as developed by Edwards [13–17] assumes that the band is infinite, therefore $s_{\min}$ goes to zero ($R \to \infty$). It is also noted that the square root term in equation (3b) is important for small values of k, while as k increases, the first two terms dominate. These observations and the desire for a $g(k)$ expression with an analytical invertable function suggest the truncation of the equation (3b) after the first two terms, such that the simplified cumulative distribution function becomes

$$g_{B\to 0,\mathrm{wb}}(k) = \begin{cases} 0 & \text{for } k < e^2 s_{\min}B \\ \dfrac{1}{\ln(R)}\left[\ln\left(\dfrac{k}{s_{\min}B}\right)-2\right] & \text{for } e^2 s_{\min}B \leqslant k \leqslant s_{\max}B \\ 1-\dfrac{2\sqrt{R}}{\ln(R)}\sqrt{\dfrac{s_{\min}B}{k}} & \text{for } s_{\max}B < k \end{cases} \tag{4a,b,c}$$

Note that the regions of application for equations (4a) and (4b) incorporate a factor of e^2 to satisfy the limits in $g(k)$, and equation (4c) is modified from equation (3c) such that the cumulative distribution function remains continuous for the entire interval, and differentiable for $k = s_{\max}B$.

Figure 2 shows the difference between the cumulative distribution function as determined with equations (3) and (4), for several values of the ratio R, for a value of the pressure broadening parameter $B = 10^{-4}$. The largest differences between the formulations occur for small values of R. For large values of R, the differences between the two expressions occur primarily for small values of the cumulative distribution function, $g(k) < 0.2$ for $R = 10^6$, with a direct impact on band absorption for large values of the optical path. Secondly, for several important bands, the actual phenomena for small values of the absorption coefficient within the band are more complex and are only approximated by this model [12]. It is noted that equations (4b) and (4c) can be analytically inverted, leading to simple, explicit expressions for the absorption coefficient.

In the large pressure limit, the narrow band models developed by Elsasser [19], Goody [20] and Malkmus [8] lead to the same result in the pressure broadened limit for the cumulative distribution function, namely

$$g_{B\to\infty,\mathrm{nb}}(k) = \begin{cases} 0 & \text{for } k < s \\ 1.0 & \text{for } k \geqslant s \end{cases} \tag{5a,b}$$

where s is the mean line intensity-to-spacing ratio within

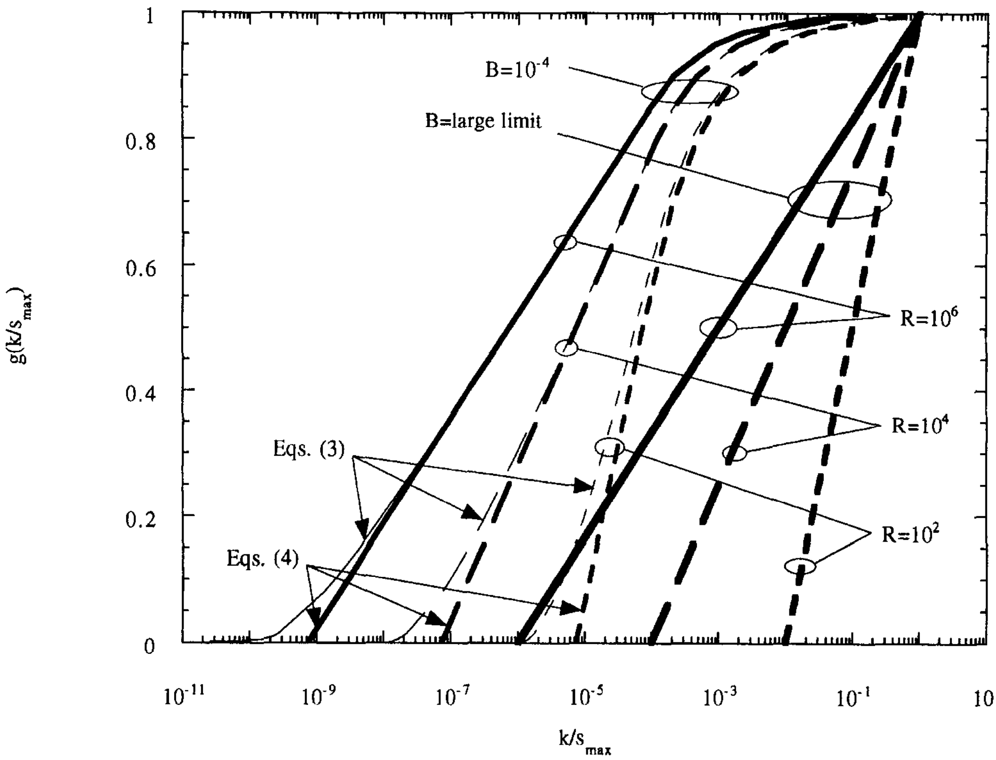

Fig. 2. Absorption coefficient cumulative distribution function for the low pressure model for $B = 10^{-4}$, as predicted by the equations (3) (plain lines) and by equations (4) (bold lines), and for the high pressure model as predicted by equations (6) (extra bold lines), for different values of R.

the band. Equations (5) and the exponential wide band model lead to an expression of the coefficient cumulative distribution function of the form

$$g_{B\to\infty,\mathrm{wb}}(k) = \begin{cases} 0 & \text{for } k < s_{\min} \\ \dfrac{\ln\left(\dfrac{k}{s_{\min}}\right)}{\ln(R)} & \text{for } s_{\min} \leqslant k \leqslant s_{\max}. \\ 1.0 & \text{for } s_{\max} < k \end{cases} \qquad \text{(6a,b,c)}$$

It is noted that the expressions in equations (6) can be analytically inverted. Figure 2 shows the absorption coefficient cumulative distribution function in the large pressure limit, for different values of the ratio R. It is noted that the cumulative distribution function is a straight line in semi-log coordinates.

2.2. Wide band cumulative distribution function

A general model is sought for the absorption coefficient cumulative distribution function for wide band intervals for all pressures. First, the derivation considers the model described by equations (3) and (6), followed by its application to the simplified approach in equation (4). The model should be continuous and exact in the limits of small and large B as prescribed by equations (3) and (6), as well as accurate for intermediate values of the pressure broadening parameter. The analysis of equations (3) and (6) shows that, while for small values of B the distribution function depends upon the ratio $k/(s_{\min}B)$, in the pressure broadening limit it only depends on $k/s_{\min}$. This suggests the replacement of these two expressions with the non-dimensional variable

$$\kappa = \frac{k}{s_{\min}(1-e^{-B})}$$

which satisfies both limits. A second observation is related to the logarithmic expressions in equations (3b) and (6b). In the pressure broadening limit the cumulative distribution function is represented by only a logarithmic expression in equation (6b). At the opposite limit defined by small values of B, two additional terms follow the logarithmic variation of the cumulative distribution function in equation (3b). This suggests the multiplication of the additional terms in equation (3b) by $e^{-B/4}$, thus, satisfying both limits. From continuity requirements, the same factor has to be applied to the square root term in equation (3c), such that equations (3) and (6) can be combined to yield

$$g_{\mathrm{wb}}(\kappa) = \begin{cases} 0 & \text{for } \kappa \leqslant 1 \\ \dfrac{1}{\ln(R)}\left[\ln(\kappa) - 2e^{-B/4}\left(1 - \dfrac{1}{\sqrt{\kappa}}\right)\right] & \text{for } 1 < \kappa \leqslant R \\ 1 - \dfrac{2e^{-B/4}}{\ln(R)}(\sqrt{R}-1)\dfrac{1}{\sqrt{\kappa}} & \text{for } R < \kappa \end{cases} \tag{7a,b,c}$$

Finally, a fitting function $W(B, R)$ is introduced for intermediate values of B. Equation (1) shows that, in the limit as $B \to 0$, the absorption coefficient is defined for the interval (sB, ∞). As the pressure broadening parameter increases, this limiting approximation becomes less accurate, overpredicting the absorption coefficient and leading to errors in the cumulative distribution function, specifically in the neighborhood of $g(k) = 1.0$. To eliminate this overprediction of the absorption coefficient, a scaling based upon a maximum value for the absorption coefficient is sought. The Elsasser narrow band model [19] provides an analytical approximation for the spectral variation of the absorption coefficient within a narrow band. Using the maximum value provided by this formulation, the model in equations (7) uses the limiting absorption coefficient within the wide band of

$$k_{\max} = s_{\max}\frac{\sinh(2\pi B)}{\cosh(2\pi B) - 1} \tag{8a}$$

and, in terms of the nondimensional variable κ, this becomes

$$\kappa_{\max} = \frac{R}{(1-e^{-B})}\frac{\sinh(2\pi B)}{\cosh(2\pi B)-1}. \tag{8b}$$

Noting that the cumulative distribution function is $g_{\mathrm{wb}}(\kappa) = 1.0$ for $\kappa = \kappa_{\max}$, and substituting equation (8b) into the $g_{\mathrm{wb}}(\kappa)$ for large κ suggests the functional dependence of

$$\frac{2e^{-B/4}}{\ln(R)}\frac{\sqrt{R}-1}{\sqrt{R}}\sqrt{\frac{(1-e^{-B})[\cosh(2\pi B)-1]}{\sinh(2\pi B)}}.$$

This dependence is zero in the limits of B going to zero and infinity and finite for intermediate values of B. This function is inversely proportional to $\ln(R)$ which implies that, in the limit $R \to \infty$, this function is equal to zero. Since for most practical applications the ratio R is relatively large so the term $(\sqrt{R}-1)/\sqrt{R} \cong 1.0$, the fitting function $W(B, R)$ is defined as

$$W(B, R) = \frac{2e^{-B/4}}{\ln(R)}\sqrt{\frac{(1-e^{-B})[\cosh(2\pi B)-1]}{\sinh(2\pi B)}}. \tag{9}$$

The resulting formulation of the absorption coefficient cumulative distribution function from equations (3) and (6) is

$$g_{\mathrm{wb}}(\kappa) = \begin{cases} 0 & \text{for } \kappa \leqslant 1 \\ W(B,R)e^{-\frac{1}{(\kappa-1)^2}} + \dfrac{1}{\ln(R)}\left[\ln(\kappa) - 2e^{-B/4}\left(1 - \dfrac{1}{\sqrt{\kappa}}\right)\right] & \text{for } 1 < \kappa \leqslant R \\ 1 + W(B,R)e^{-\frac{1}{(\kappa-1)^2}} - \dfrac{2e^{-B/4}}{\ln(R)}(\sqrt{R}-1)\dfrac{1}{\sqrt{\kappa}} & \text{for } R < \kappa \leqslant \kappa_{\max} \\ 1.0 & \text{for } \kappa_{\max} < \kappa \end{cases} \tag{10a,b,c,d}$$

where the exponential function that multiplies $W(B, R)$ is introduced to ensure the convergence of the cumulative distribution function to zero for small values of the absorption coefficient, as well as the function continuity.

The expressions in equations (10) have the inconvenience of not being invertable, therefore the absorption coefficient cannot be explicitly defined. In order to obtain explicit expressions for the wide band absorption coefficient distribution, the same development as above is performed for the simplified expressions in equations (4) and (6). In this case, the cumulative distribution function yields

$$g_{\mathrm{wb}}(\kappa) = \begin{cases} 0 & \text{for } \kappa \leqslant e^{2e^{-B/4} - W(B,R)\ln(R)} \\ W(B,R) + \dfrac{1}{\ln(R)}[\ln(\kappa) - 2e^{-B/4}] & \text{for } e^{2e^{-B/4} - W(B,R)\ln(R)} < \kappa \leqslant R \\ 1 + W(B,R) - \dfrac{2e^{-B/4}}{\ln(R)}\sqrt{\dfrac{R}{\kappa}} & \text{for } R < \kappa \leqslant \kappa_{\max} \\ 1.0 & \text{for } \kappa_{\max} < \kappa \end{cases} \tag{11a,b,c,d}$$

and after performing the analytical inversion, the non-dimensional absorption coefficient results as

$$\kappa = \begin{cases} e^{[g_{\mathrm{wb}}(\kappa) - W(B,R)]\ln(R) + 2e^{-B/4}} \\ \qquad \text{for } 0 \leqslant g_{\mathrm{wb}}(\kappa) \leqslant 1 + W(B,R) - \dfrac{2e^{-B/4}}{\ln(R)} \\ R\left[[1 + W(B,R) - g_{\mathrm{wb}}(\kappa)]\dfrac{\ln(R)}{2e^{-B/4}}\right]^{-2} \\ \qquad \text{for } 1 + W(B,R) - \dfrac{2e^{-B/4}}{\ln(R)} < g_{\mathrm{wb}}(\kappa) \leqslant 1.0 \end{cases} \qquad (12\text{a,b})$$

It is noted that in equations (11) and (12), the exponential function multiplying the function $W(B, R)$ in equations (10) is not necessary due to the monotonicity of equations (4), as opposed to equation (3). Also, the function $W(B, R)$ in equation (9), which results as an approximation from equations (3), is exact when calculated from equations (4). Equations (10) and (12) represent the proposed model for the absorption coefficient distribution for wide spectral intervals. The differences between the more complete model in equations (10) and the simplified model in equations (12) occur for relatively small values of the absorption coefficient. For short optical paths, small absorption coefficients yield very small optical depths so the transmissivity approaches unity and the absorptivity approaches zero. As the optical path increases, even small values of the absorption coefficient are important to radiative transport and equations (10) are more appropriate. Figure 2 also shows that, as the ratio between the maximum and minimum line intensity-to-spacing ratio decreases, the differences between the complete and approximate formulations increase.

It is concluded that the model expressed by equations (10)–(12) is exact in the limits of small and large values of the pressure broadening parameter and accurate for intermediate values of B. Figure 3 shows the variation of the absorption coefficient cumulative distribution function for a wide range of pressure broadening parameters B, for a fixed value $R = 10^6$, as described by equations (10) and (12). The plain lines show the results obtained with the complete model as presented in equations (10), while the bold lines are obtained with equations (12). The simplified model predicts somewhat larger values of the absorption coefficient for the low values of the cumulative distribution function. The application of these models to water vapor shows that although the complete formulation improves the overall accuracy of the model, the simplified model is in good agreement with the exact calculations. Figure 3 also shows that for the simplified

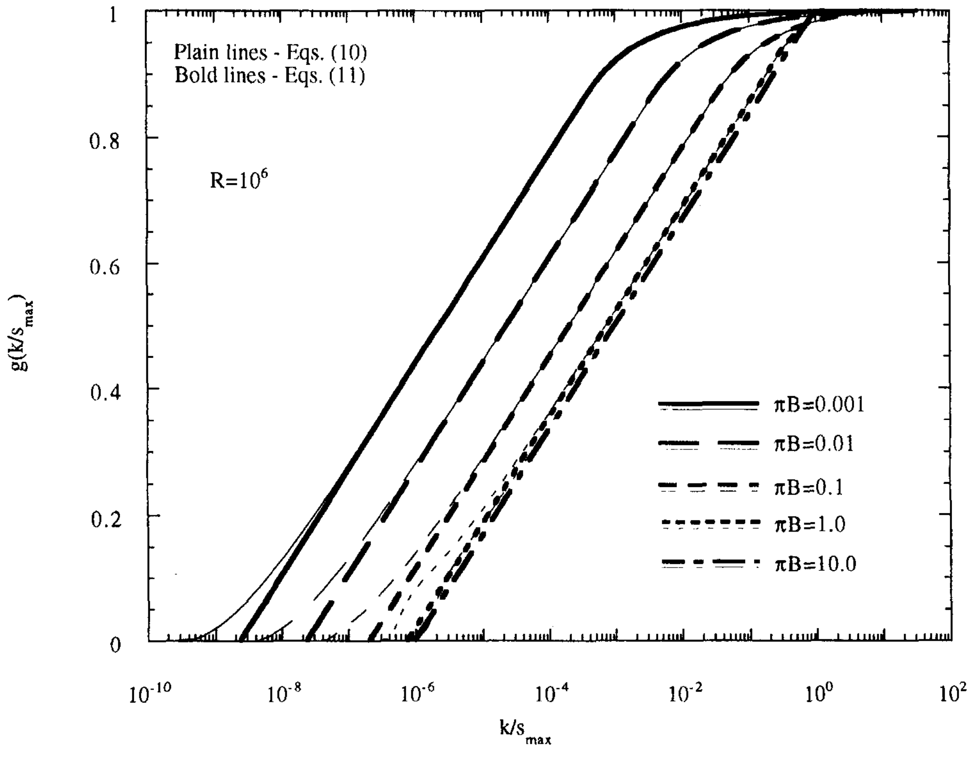

Fig. 3. Absorption coefficient cumulative distribution function as resulted from equations (10)—plain lines, and from equations (11) and (12)—bold lines, for different values of the pressure broadening parameter.

model as described by equations (12), the variation is linear in semi-log coordinates for small values of the absorption coefficient and asymptotes to $g(k) = 1$ as the absorption coefficient increases. The asymptotic region determined by equation (12b) diminishes as the pressure broadening parameter B increases. The accuracy of the proposed model when applied to actual bands is discussed below.

3. Band parameters for H_2O

This work is directed towards the derivation of improved cumulative distribution function band parameters for the rotational–vibrational bands of water vapor. The availability of reliable line-by-line spectral data for ambient temperatures and up to 1500 K [1, 2] permits the determination of accurate band parameters only for this temperature range. Many engineering applications require accurate calculations for a wider range of temperatures, for which line-by-line data is not readily available. For such temperatures, recent developments [3] using accurate band models may be accessed. This work uses the band parameters as developed by Soufiani and Taine [3] for the Malkmus narrow band model. Wide band parameters are then generated to minimize the differences between the wide band absorption coefficient cumulative distribution functions obtained with the narrow band results and the proposed model. The spectral lower limit ν_l, upper limit ν_u and the spectral interval $\Delta\nu = \nu_u - \nu_l$ are set for each band and maintained for all pressures and temperatures. The band spectral limits are presented in Table 1. This procedure is different from the original formulation of the wide band model [13–17], where the band limits are not specifically required. The original wide band model calculates the wide band absorption, which for a given pathlength becomes independent of the band spectral magnitude. The proposed model attempts to determine specific values of the absorption coefficient within the band, and is dependent upon the spectral interval considered. As the spectral interval widens, the corresponding distribution function shifts towards smaller values of the absorption coefficient.

The cumulative distribution functions for temperatures between 300 and 2900 K are calculated for the 1.38, 1.87, 2.7 and 6.3 μm bands, and between 300 and 1900 K for the rotational band, for all increments of 200 K. It is noted that for elevated temperatures, the rotational band contribution to the thermal energy transport is negligible. The total pressure and the partial pressure of water vapor are equal, and they vary between 0.01 and 10.0 atm in powers of 10. For each distinct cumulative distribution function, 32 values of the absorption coefficient corresponding to the Gaussian quadrature locations are obtained. The root mean square (RMS_k) of the differences defined as

$$\delta_k = \frac{k_e - k_m}{k_e} \tag{13}$$

is minimized, where k_e is the exact absorption coefficient from the line-by-line or narrow band model calculations [2, 3], and k_m is the absorption coefficient from the proposed simplified model [equations (12)] for the same temperatures, pressures and cumulative distribution function values. The band parameters describing the band intensity α [13, equation (78)], the bandwidth parameter ω [13, equation (95)] and the broadening parameter β [13, equation (99)] are adjusted to accurately describe the absorption coefficient cumulative distribution function. It is noted that the broadening parameter β is used to calculate the pressure broadening parameter $B = \beta P_e$, where P_e is the effective pressure [13, equation (58)]. Note

Table 1
The water vapor band parameters for use in equations (12)

Band [μm]	ν_l [cm^{-1}]	ν_u [cm^{-1}]	Transition	α_0[a] [cm^{-1} g^{-1} m^2]	β_0[a,b]	ω_0[a] [cm^{-1}]
1.38	6000	8000	1,0,1	2.17	0.1180	78.0
1.87	4400	6000	0,1,1	2.64	0.0850	70.6
2.7	2600	4400	0,2,0	0.19[c]	0.0360[d]	83.0
			1,0,0	2.30[c]		
			0,0,1	23.3[c]		
6.3	1000	2600	0,1,0	39.6	0.0566	72.8
Rotational	150	1000	0,0,0	420.0[e]	0.1140	37.0

[a] Use with temperature and pressure dependencies in ref. 13.

[b] For all bands, $b_B = 8.6\sqrt{T/T_0} + 0.5$ and $n = 1$ in P_e with $T_0 = 100$ K and $P_0 = 1$ atm.

[c] $\alpha_{2.7} = \Sigma_{j=1}^{3} \alpha_j$.

[d] $\gamma_{2.7} = (1/\alpha_{2.7})\left(\Sigma_{j=1}^{3} \sqrt{\alpha_j \gamma_j}\right)^2$.

[e] Use equation (14) for temperature dependence.

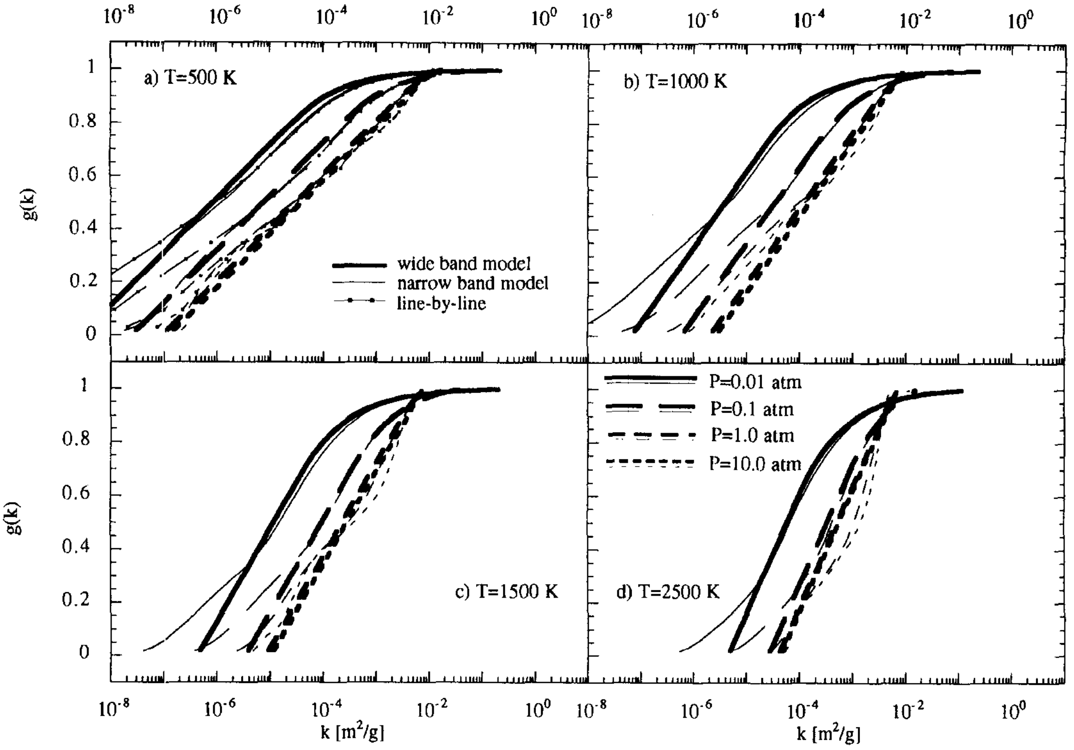

Fig. 4. Absorption coefficient cumulative distribution function for the 1.38 μm band of water vapor, for (a) $T = 500$ K, (b) $T = 1000$ K, (c) $T = 1500$ K and (d) $T = 2500$ K, for different pressures. The plain lines represent the narrow band model results [3, 4], the bold lines represent the simplified wide band model as described by equations (12) and the marked lines in (a) represent the line-by-line results [2].

that Edwards [13] uses a pressure broadening parameter π times larger than the pressure broadening parameter B used here.

Figures 4–8 present the cumulative distribution functions for the investigated bands, using the benchmark distributions together with the proposed model expressed by equations (12) with the parameters in Table 1. Figures 4–7 present the results obtained for the 1.38, 1.87, 2.7 and 6.3 μm band, respectively, for temperatures between 500 and 2500 K, using the equations (12) and the narrow band model results for the same pressure range noted above. Additionally, Figs. 4(a)–7(a) show the absorption coefficient cumulative distribution functions obtained with the line-by-line database [2]. The line-by-line results are in good agreement with the narrow band results, supporting the use of these results in Figs. 4–7 and in model development. It is noted that the proposed model is in good agreement with the narrow band model and the exact calculations for large domains of the cumulative distribution functions. Differences occur for small values of the absorption coefficient, and some differences can be observed for large pressures, indicating the limitations of the exponential wide band model. The band absorptivity study presented below shows that the small values of the absorption coefficient often have a minor influence on the typical heat transfer characteristics. Figure 8 shows the absorption coefficient cumulative distribution functions of the rotational band, for temperatures of 500, 1000, 1500 and 1900 K and for pressures of 0.01–10 atm. Figure 8(a) compares the proposed model (wide band model) with the line-by-line results [1, 2] for a temperature of 500 K. Figures 8(b)–(d) show the proposed model together with the narrow band model, as predicted by Soufiani and Taine [3, 4], for temperatures of 1000, 1500 and 1900 K, respectively. Although the overall variation of the rotational band cumulative distribution function is generally accurate, differences between the methods occur as indicated by the magnitude of the root mean square error discussed below, primarily for elevated temperatures. The proposed band parameters for the rotational band can be used for temperatures higher than 1900 K, with increased differences when compared to benchmark calculations.

The results presented in Figs. 4–8 use the new band parameters α_0, β_0 and ω_0 presented in Table 1 and the simplified model presented in equations (12). It is noted that there are three interacting transitions for the 2.7 μm band which are combined according to the prescriptions

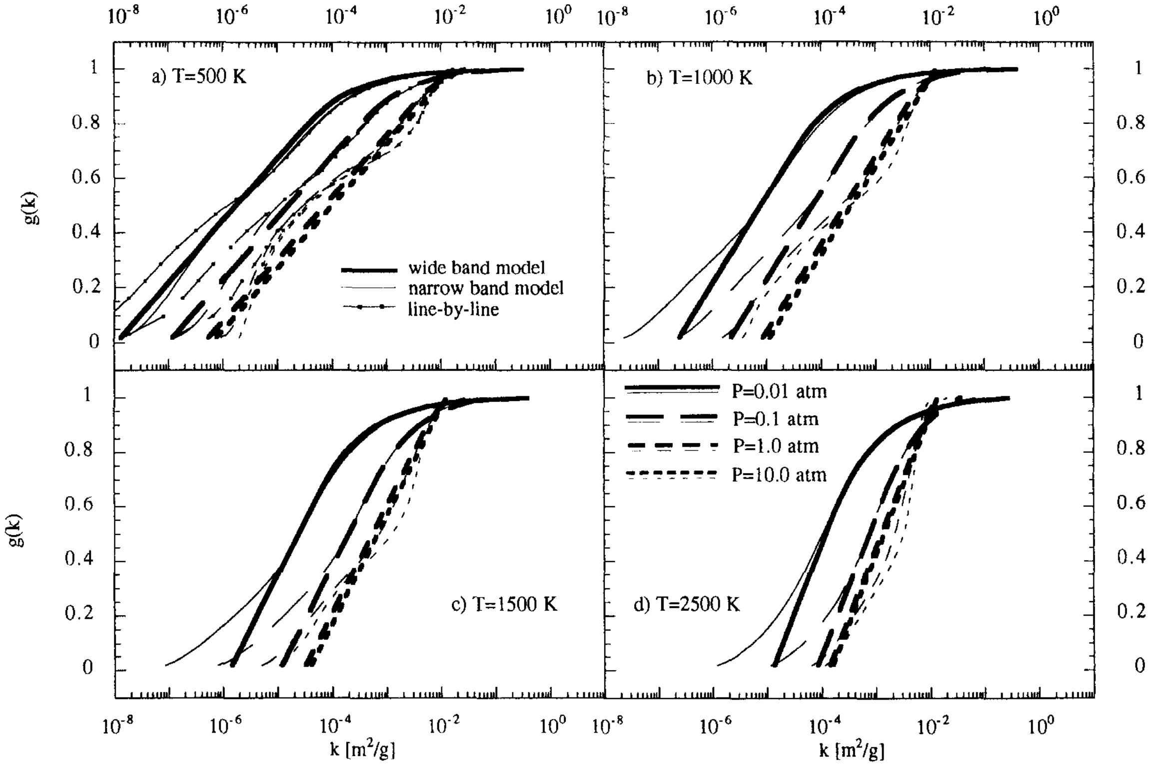

Fig. 5. Absorption coefficient cumulative distribution function for the 1.87 μm band of water vapor, for (a) $T = 500$ K, (b) $T = 1000$ K, (c) $T = 1500$ K and (d) $T = 2500$ K, for different pressures. The plain lines represent the narrow band model results [3, 4], the bold lines represent the simplified wide band model as described by equations (12) and the marked lines in (a) represent the line-by-line results [2].

of Edwards [13–17]. The new band parameters were determined by minimizing the root mean square error of the cumulative distribution functions for the wide intervals of temperature and pressure noted above. The RMS_k is calculated using absorption coefficients corresponding to $g(k)$ greater than 0.2. This procedure is justifiable by noting that, for $g(k) < 0.2$ there correspond relatively small values of the absorption coefficient which are of less importance for many engineering applications. In addition, the small absorption coefficient region of the cumulative distribution function originates primarily in the band wings, which are not exhaustively studied to date, particularly for high temperatures. For example, Hartmann et al. [21] perform calculations and measurements in the band wings of the 2.7 and 6.3 μm H_2O bands up to 900 K, showing that the errors in existing calculations are mostly due to inaccuracies in the theoretical models. Comparisons between different widely used methods such as line-by-line and narrow band models show significant differences in the absorption coefficient magnitudes in the band wings for various conditions, primarily for small pressures of the absorbing gas.

The temperature variation of the parameter α as proposed by Edwards [13, 14] is preserved for the 1.38, 1.87, 2.7 and 6.3 μm bands. For the rotational band the optimized variation of the band intensity parameter is found to be

$$\alpha(T) = \alpha_0 \exp(-3\sqrt{100/T}) \qquad (14)$$

where T [K] is the gas temperature. It is noted that Edwards proposes a factor of five multiplying the square root term in equation (14), while Modak [22] proposes a factor of nine. The optimized parameters α_0 are presented in Table 1 for all bands, together with equation (14) for the rotational band. The bandwidth parameter temperature variation as proposed by Edwards is preserved in the optimization process with the new values of ω_0 presented in Table 1 for all bands. The temperature variation of β as proposed by Edwards [13, 14] is also preserved, and the optimized values of β_0 are presented in Table 1. The results show that the band parameters are generally of the same order of magnitude as the original parameters presented by Edwards. The only notable difference is in the parameter α_0 for the rotational band which is two orders of magnitude smaller than the original value prescribed by Edwards, primarily due to the

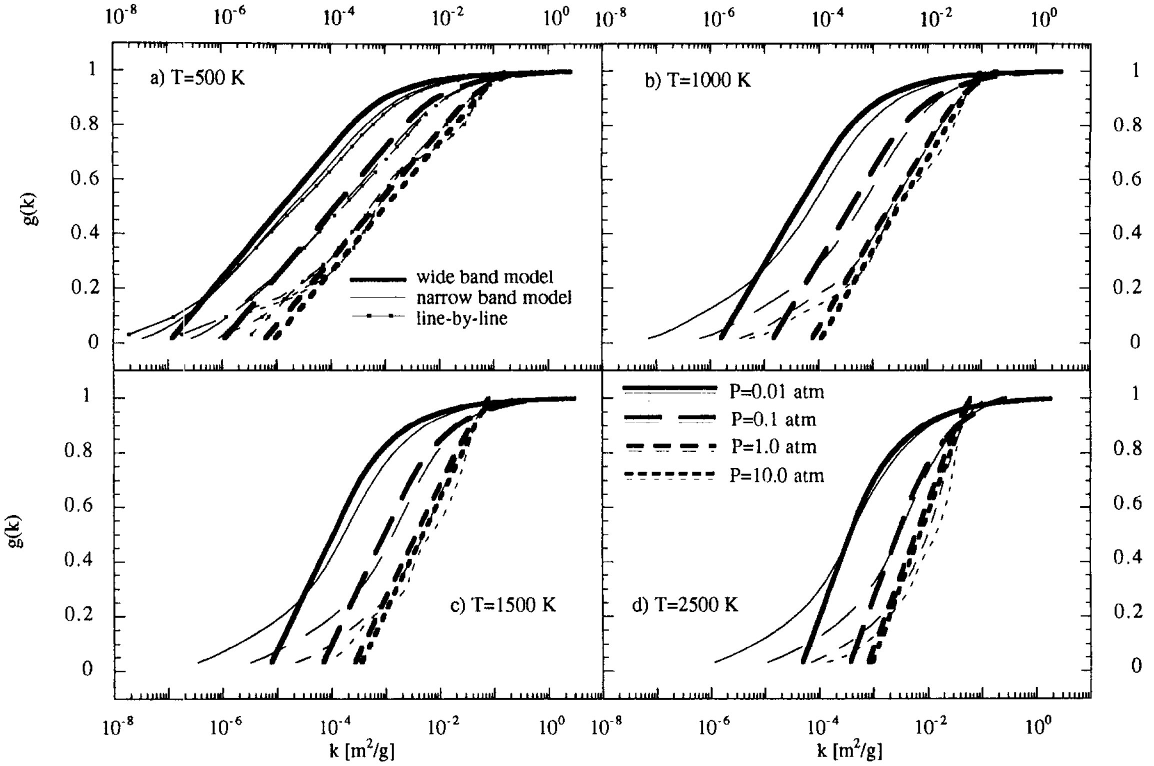

Fig. 6. Absorption coefficient cumulative distribution function for the 2.7 μm band of water vapor, for (a) $T = 500$ K, (b) $T = 1000$ K, (c) $T = 1500$ K and (d) $T = 2500$ K, for different pressures. The plain lines represent the narrow band model results [3, 4], the bold lines represent the simplified wide band model as described by equations (12) and the marked lines in (a) represent the line-by-line results [2].

new formulation of the line intensity parameter in equation (14).

Table 2 shows the root mean square error ($\mathrm{RMS_k}$) obtained with the simplified model in equations (12), together with the root mean square error ($\mathrm{RMS_{k,c}}$) obtained for the more complete model in equations (10). The values presented in Table 2 are obtained using absorption coefficients corresponding to cumulative distribution functions $g(k) > 0.2$. Table 2 shows that the rotational band model introduces more significant errors than the other bands. Similar error characteristics are mentioned by Edwards [13–17] and Modak [22]. It is also noted that the errors introduced by the relatively weak bands centered at 1.38 and 1.87 μm are somewhat larger than the stronger bands centered at 2.7 and 6.3 μm. The magnitudes of the root mean square error for all bands based upon $g(k) > 0.2$ show that the wide band model accurately describes the absorption coefficient distribution function. Note that the errors based upon all values of $g(k)$ (i.e., $0 \leqslant g(k) \leqslant 1.0$) will be significantly higher, mainly due to more substantial differences in the small regions of the distribution functions. The more complete model expressed by equations (10) is also compared to the benchmark calculations using the same band parameters, with relatively small $\mathrm{RMS_k}$ differences from the results given by equations (12). It is noted that the model described by equations (10) differs from the model in equations (12) for small values of the cumulative distribution function. This implies that the differences in the absorptivity calculated with the two models will occur at large optical paths. Finally, the results presented in Table 2 indicate that the fitting function $W(B, R)$ is useful in describing the k-distribution function for intermediate values of the pressure broadening parameter B.

4. Wide band absorption comparisons

The different band models are often used to calculate the gas absorption over specified spectral intervals. The wide band absorption A quantifies the wide band absorptivity and is defined as

$$A = \int_{\Delta\nu} (1 - e^{-k(\nu)u})\,\mathrm{d}\nu \tag{15}$$

where $\Delta\nu$ is the wide band spectral interval and u is the

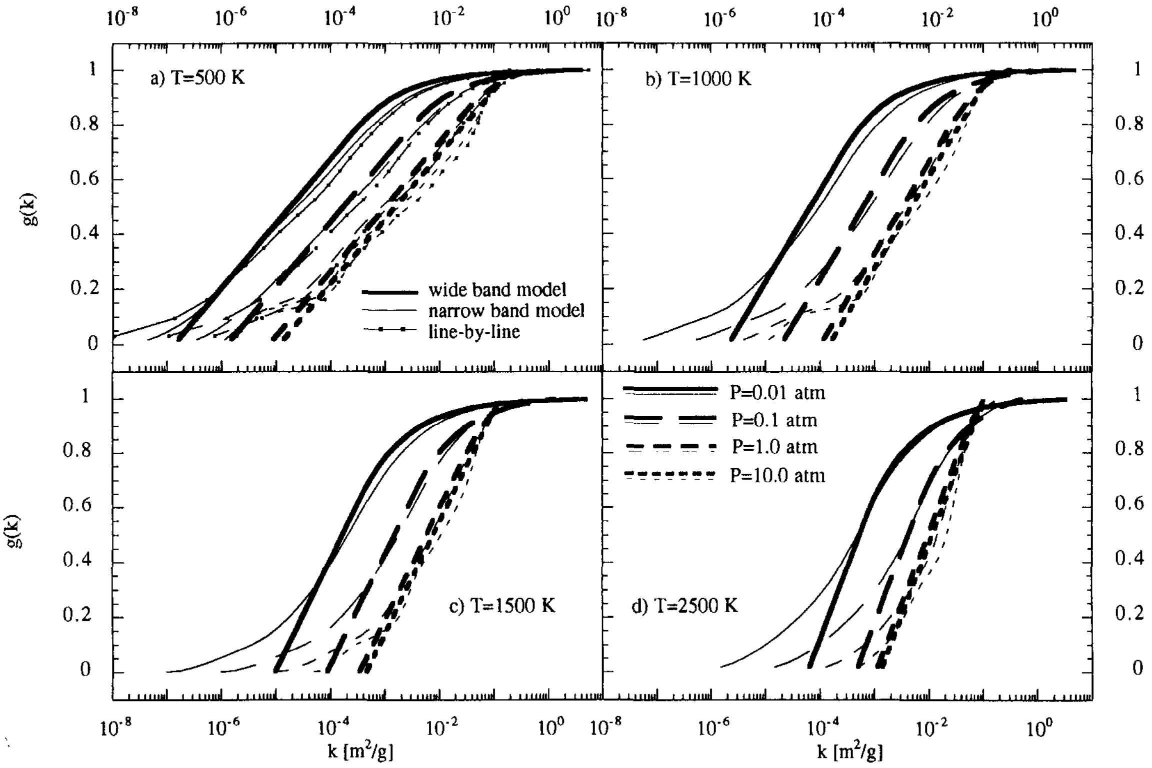

Fig. 7. Absorption coefficient cumulative distribution function for the 6.3 μm band of water vapor, for (a) $T = 500$ K, (b) $T = 1000$ K, (c) $T = 1500$ K and (d) $T = 2500$ K, for different pressures. The plain lines represent the narrow band model results [3, 4], the bold lines represent the simplified wide band model as described by equations (12) and the marked lines in (a) represent the line-by-line results [2].

mass pathlength, $u = \rho L$, defined as the product between the absorbing gas density ρ and the optical length L. The integral over the spectral interval $\Delta\nu$ can be replaced with an integral over the absorption coefficient cumulative distribution function as

$$A^* = A/\omega = \frac{\Delta\nu}{\omega}\int_0^1 (1-e^{-ku})\,\mathrm{d}g_{\mathrm{wb}} \tag{16}$$

and can be calculated

$$A^* = \frac{\Delta\nu}{\omega}\sum_{i=1}^{N}(1-e^{-k_i u})w_i \tag{17}$$

where N_q is the number of quadratures in the summation, w_i are the weights and k_i are the correspondent absorption coefficients.

The model and the band parameters developed above for the water vapor bands [equations (10) and (12) with Table 1] are used to calculate the band absorption. The number of quadratures $N_q = 32$ is used for the following calculations. It is noted that as B increases, the number of quadratures can be decreased. A reduced number of quadratures can be used for small pressures using different integration schemes [3]. The mean root square error RMS_A is defined as

$$\delta_A = \frac{A_e^* - A_m^*}{A_e^*} \tag{18}$$

and is calculated for each band, for particular values of temperature, pressure and optical length. A_m^* values are calculated using equations (12) or equations (10) together with the band parameters in Table 1, and A_e^* values are obtained from line-by-line or narrow band model calculations.

Table 2 shows the root mean square error for the wide band absorption RMS_A, for temperatures in the ranges 300–2900 K for the rotational–vibrational bands and 300–1900 K for the rotational band. The pressures include 0.01–10 atm. For each set of temperatures and pressures, the wide band absorption as expressed in equation (17) is calculated for a wide range of geometric paths, between 10^{-3} and 10^3 meters. The RMS_A error values are less than 14% for the weaker bands, the 1.38 and 1.87 μm bands, approximately 12% for the 2.7 and the 6.3 μm bands and 16% for the rotational band. It is noted that the RMS_A results obtained with equations (12) and with

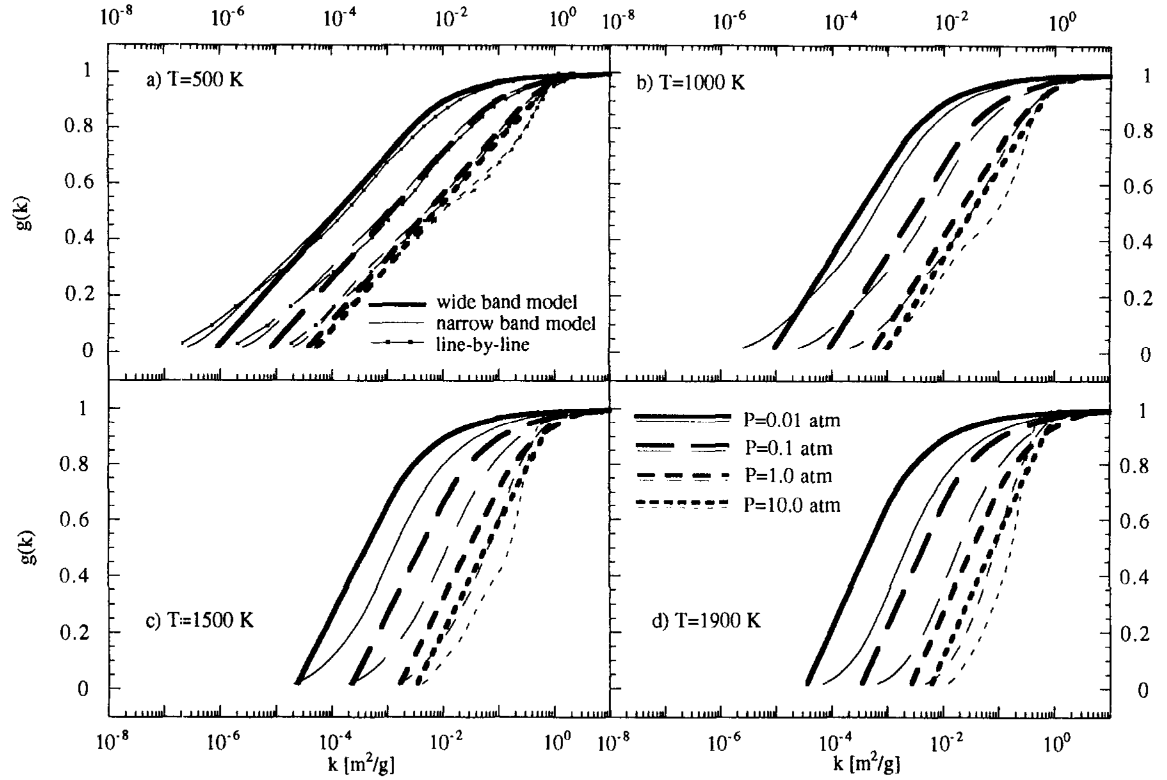

Fig. 8. Absorption coefficient cumulative distribution function for the rotational band of water vapor, for (a) $T = 500$ K, (b) $T = 1000$ K, (c) $T = 1500$ K and (d) $T = 1900$ K, for different pressures. The plain lines represent the narrow band model results [3, 4], the bold lines represent the simplified wide band model as described by equations (12) and the marked lines in (a) represent the line-by-line results [2].

Table 2
Root mean square error for the absorption coefficient for $g(k) > 0.2$ and the wide band absorption for temperatures between 300 and 2900 K (1900 K for the rotational band), and pressures between 0.01 and 10 atm

Band [μm]	RMS_k [%]	$\mathrm{RMS}_{k,c}$ [%]	RMS_A [%]	$\mathrm{RMS}_{A,c}$ [%]
1.38 μm	41.6	32.6	14.2	15.5
1.87	45.1	37.8	13.1	14.0
2.7	26.4	23.0	12.5	14.6
6.3	27.2	24.1	12.5	12.3
Rotational	49.7	46.5	16.1	16.5

equations (10) are similar, suggesting the relatively small importance of the small values of the absorption coefficient within the distribution to the wide band absorption, even for relatively large values of the optical path. The results obtained with the line-by-line calculations [1, 2] for temperatures up to 1000 K provide essentially the same values with the results obtained with the narrow band database [3, 4]. The results reported in Table 2 use the narrow band model database, in order to obtain the desired temperature range.

Table 3 (top four rows) shows the average difference δ_A between the wide band absorption obtained using the narrow band model and the simplified model in equation (12) for individual temperatures, for the entire pressure range, and the indicated geometric path range. Two different path ranges have been selected, 10^{-3}–10^{3} meters and 10^{-1}–10^{3} meters, respectively. This choice of pathlengths is used to indicate the larger errors that occur for very small values of the optical length. This phenomenon, experienced by numerous other researchers ([5, 7, 10]), does not have a significant impact on the solution of the radiative transfer equation due to the small values of absorption. Table 3 shows that the errors between 10^{-1}–10^{3} meters are generally less than 9% for the 1.38, 1.87, 2.7 and 6.3 μm bands for the entire temperature range considered and for the rotational band at low temperatures. The errors are larger for the rotational band at high temperatures. The errors occurring for the interval 10^{-3}–10^{3} meters are relatively higher, but not higher than 10% for the 2.7 and 6.3 μm bands and 16% for the other

Table 3

Average difference of the wide band absorption for the five water vapor bands [equations (12)] for the indicated temperatures and range of pathlengths, and for pressures in the range 0.01–10.0 atm (rows 1–4), and average difference for the same bands for the indicated pressures and range of pathlengths, and for temperatures in the range 300–2900 K for the 1.38, 1.87, 2.7 and 6.3 micron bands, and 300–1900 K for the rotational band (rows 5–8)

	$\bar{\delta}_{A\ 1.38\ \mu m\ band}$ [%]		$\bar{\delta}_{A\ 1.87\ \mu m\ band}$ [%]		$\bar{\delta}_{A\ 2.7\ \mu m\ band}$ [%]		$\bar{\delta}_{A\ 6.3\ \mu m\ band}$ [%]		$\bar{\delta}_{A\ rotational\ band}$ [%]	
T [K] P [atm]	10^{-3}–10^{3} [m]	10^{-1}–10^{3} [m]	10^{-3}–10^{3} [m]	10^{-1}–10^{3} [m]	10^{-3}–10^{3} [m]	10^{-1}–10^{3} [m]	10^{-3}–10^{3} [m]	10^{-1}–10^{3} [m]	10^{-3}–10^{3} [m]	10^{-1}–10^{3} [m]
$T = 500$	10.7	8.2	10.0	7.7	9.0	8.3	9.2	7.5	3.1	5.9
$T = 1000$	12.3	10.1	12.0	9.8	10.4	8.8	9.7	7.7	8.2	9.0
$T = 1500$	11.4	9.6	11.5	9.4	10.7	8.6	9.6	6.6	16.0	15.3
$T = 2500$	10.7	8.8	8.9	7.6	9.6	6.6	9.1	6.7	na	na
$P = 0.01$	17.0	13.9	18.1	14.1	14.8	13.4	17.6	13.1	23.1	19.9
$P = 0.1$	8.4	6.8	7.7	6.5	8.6	7.3	10.7	7.8	13.5	14.2
$P = 1.0$	11.6	9.4	9.4	7.8	9.6	6.9	5.7	4.4	4.4	6.1
$P = 10.0$	7.7	6.7	6.2	5.8	6.4	3.8	3.4	2.6	1.0	4.6

bands. The 6.3 μm band generally yields slightly smaller errors when compared to the 2.7 μm band. This behavior may be attributed to the different superposition of the dominant vibrational transitions within the wide band. While the 6.3 μm band has one single dominant vibrational transition, the 2.7 μm band is dominated by three interacting vibrational transitions on the spectral interval considered (described in Table 1).

Table 3 (bottom four rows) presents the error $\bar{\delta}_A$ for several pressures, averaged over temperatures up to 2900 K for the rotational–vibrational bands and 1900 K for the rotational band, and the same range of the pathlengths as noted above. It can be observed that for a pressure of 0.01 atm, the average difference for the path interval of 10^{-3}–10^{3} meters is less than 23%, and the difference rapidly decreases as the pressure increases to below 10%. For the path interval of 10^{-1}–10^{3} meters and pressures larger than 0.1 atm, the errors are generally below 7% for all bands, excluding the rotational band. It is noted that the wide band absorption errors are of the same order of magnitude with the values reported by Edwards [13]. It is concluded that the simplified model accurately predicts the band absorptivity over large ranges of temperatures, pressures and optical paths, and the largest errors occur for regions where the wide band absorption is small.

The wide band absorption obtained with the simplified model is compared to results obtained with existing methods. Equation (17) is used to calculate the wide band absorption A^* for different values of B and a wide range of mass optical paths. The values k_i are provided by the proposed model described by equations (12) in the limit of $R \to \infty$ (used $\ln(R) = 10.0$). Figure 9 shows the variation of the wide band absorption for a wide range of optical paths and pressure broadening parameters πB. The curves have been obtained by using the wide band absorption as developed by Wang [23] for the exponential model applied to the Malkmus narrow band model, the Felske and Tien [24] model obtained from the exponential wide band model applied to the Goody narrow band model, the wide band absorption proposed by Edwards [13], and the present model [equations (12)]. The largest differences between the proposed model and Felske and Tien results are 15%, for $\pi B = 0.01$ and small values of the optical path, while the mean difference is less than 3% for the cases considered. The results obtained with the present model for intermediate values of the mass optical path are generally larger than the models of Wang, and Felske and Tien, but smaller than the values predicted by Edwards. This observation is in agreement with the results obtained for narrow band models in that the single line narrow band model predicts a higher absorptivity than the multi-line models for intermediate pathlengths. The results presented in Fig. 9 provide additional support for the approximations introduced for intermediate values of the pressure broadening parameter B by the function $W(B, R)$.

Finally, a comparison between the absorptivities obtained with the simplified model and the wide band model developed by Edwards is performed for specific water vapor bands (i.e., R finite), for pathlengths between 10^{-3} and 10^{3} meters. Such a comparison indicates the differences in the Edwards model and this model based upon the more recent databases [1–4]. An average RMS_A over the 1.38, 1.87, 2.7 and 6.3 μm bands shows that, while the simplified model [equations (12)] introduces an average of 13.1% difference, the Edwards model yields an average difference of 20.7%. When the RMS_A differ-

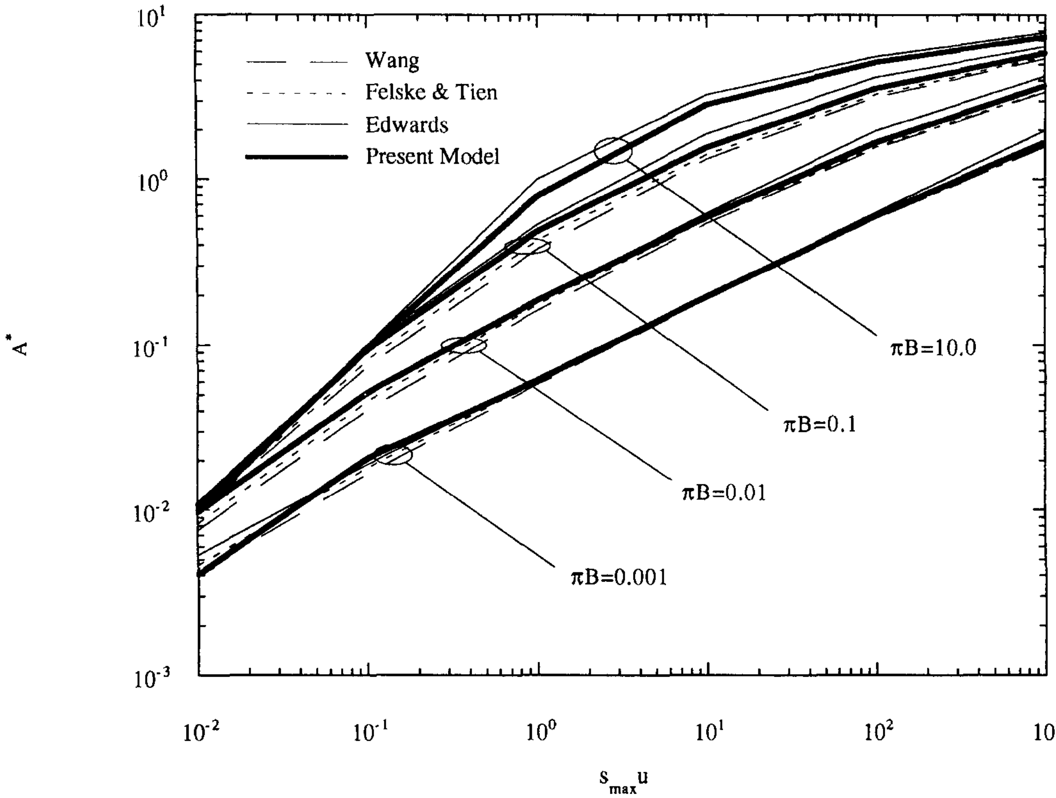

Fig. 9. Wide band absorption A^* as resulted from Wang [23], Felske and Tien [24], Edwards [13] and the simplified wide band model in equations (12), for different values of B and different optical paths.

ence is calculated for all water vapor bands (rotational band included), the values are 13.7% for the simplified model and 35.7% for the Edwards model. These differences result from the use of different benchmarks and also from the way the band spectral limits are set. The wide band $g(k)$ formulation specifies the band spectral limits and thus the different bands remain distinct in all cases, while in the original formulation [13–17] the bands have variable spectral intervals, which eventually overlap for large values of the pathlength.

5. Conclusions

This work develops a model for the absorption coefficient cumulative distribution function for large spectral intervals, corresponding to entire rotational–vibrational bands. The model is exact in the pressure broadening limit and is based on a single absorption line formulation in the small pressure limit. The model, together with an approximate function for intermediate pressures, provides a continuous formulation for the absorption coefficient cumulative distribution function. A simplified model is developed to explicitly calculate the absorption coefficient as a function of the cumulative distribution function [equations (12)]. An alternate expression of the cumulative distribution function as a function of the absorption coefficient is also proposed to improve the accuracy for small values of the absorption coefficient [equations (10)]. Although equations (10) reduce the overall error compared to equations (12), the relatively small differences in the absorption coefficient root mean square error between these models (Table 2) suggest the use of the simplified, invertable model in equations (12). It is noted that the largest errors introduced by the model when compared to the benchmark results occur for small absorption coefficients within the band, originating predominantly from the band wings, where improvements in the theoretical models are required [21].

The proposed model is applied to water vapor. Band parameters for the rotational–vibrational bands are developed. This work adjusts the wide band parameters α_0, β_0 and ω_0 for use in the absorption coefficient cumulative distribution function in equation (12), while preserving the variation of the band parameters with respect to pressure and temperature as prescribed by Edwards [13, 14]. The model introduces spectral boundaries for the water vapor bands that are maintained constant for all conditions. This assumption permits the determination of the effective absorption coefficient distribution functions that are important for calculations of general radiative transport. The proposed parameters are determined by minimizing the root mean square error between the model and the benchmark absorption coefficient cumulative distribution function of a side range of pressures and temperatures. The results show that the model accurately predicts the absorption coefficient cumulative distribution function.

The wide band absorption calculated with the proposed model is compared to existing results, with good agreement for a wide range of the pressure broadening parameter and mass optical path. The wide band absorption is also calculated using the simplified model and the recommended band parameters, and compared to line-by-line calculations for the water vapor bands. The results show the model accurately calculates the band absorption. Larger errors occur for very small optical paths, where the band absorption is very small. As the geometric path increases, the band absorption results are very good.

The simplified model together with the recommended band parameters can be used for accurate transport calculations over large spectral intervals for water vapor in both homogeneous and nonhomogeneous media. Such an absorption coefficient model is needed in problems where scattering is important. The explicit expressions of the absorption coefficient reduce the computational burden in the solution of the radiative transfer equation. Future work will be required to improve the model parameters with alternative variations of the band parameters with pressure and temperature.

Acknowledgement

This research was supported, in part, by the Richard W. Kritzer Fund.

References

[1] Rothman LS, Gamache RR, Tipping RH, Rinsland WW, Smith MAH, Benner DC, Malathy Devi V, Flaud J-M, Camy-Peyret C, Perrin A, Goldman A, Massie ST, Brown LR, Toth RA. The HITRAN molecular database: editions of 1991 and 1992. J Quant Spectrosc Radiat Transfer 1992;48:469–507.

[2] Rothman LS. HITRAN Newsletter 1996;5:1–4.

[3] Soufiani A, Taine J. High temperature gas radiative property parameters of statistical narrow-band model for H_2O, CO_2 and CO, and correlated-*k* model for H_2O and CO_2. International Journal of Heat and Mass Transfer 1997;40:987–91.

[4] Soufiani A, Taine J. Private communication.

[5] Goody R, West R, Chen L, Crisp D. The correlated-*k* method for radiation calculations in nonhomogeneous atmospheres. J Quant Spectrosc Radiat Transfer 1989;42:539–50.

[6] Marin O, Buckius RO. Wide band correlated-*k* approach to thermal radiative transport in nonhomogeneous media. Journal of Heat Transfer 1997;119:719–29.

[7] Marin O, Buckius RO. Wideband correlated-*k* method applied to absorbing, emitting and scattering media. J Thermoph Heat Transfer 1996;10:364–71.

[8] Malkmus W. Random Lorentz band model with exponential-tailed s^{-1} line-intensity distribution function. J Opt Soc America 1967;57:323–9.

[9] Domoto GA. Frequency integration for radiative transfer problems involving homogeneous non-gray gases: the inverse transmission function. J Quant Spectrosc Radiat Transfer 1974;14:935–42.

[10] Lee PYC, Hollands KGT, Raithby GD. Reordering the absorption coefficient within the wide band for predicting gaseous radiant exchange. Journal of Heat Transfer 1996;118:394–400.

[11] Parthasarathy G, Chai JC, Patankar SV. A simple approach to non-gray gas modeling. Numerical Heat Transfer, Part B 1996;29:113–23.

[12] Marin O, Buckius RO. A model of the cumulative distribution function for wide band radiative properties, forthcoming in J Quant Spectrosc Radiat Transfer.

[13] Edwards DK. Molecular gas band radiation. Adv Heat Transfer 1976;12:115–94.

[14] Edwards DK. Radiation Heat Transfer Notes. New York: Hemisphere Publishing Company, 1981.

[15] Edwards DK, Menard WA. Comparison of models for correlation of total band absorption. Appl Optics 1964;3:621–6.

[16] Edwards DK, Balakrishnan A. Thermal radiation by combustion gases. International Journal of Heat and Mass Transfer 1973;16:25–40.

[17] Edwards DK. Radiation interchange in a nongray enclosure containing an isothermal carbon-dioxide–nitrogen gas mixture. Journal of Heat Transfer 1962;84:1–11.

[18] Plass GN. Models for spectral absorption. J Opt Soc America 1958;48:690–703.

[19] Elsasser WM. Heat Transfer by Infrared Radiation in the Atmosphere, Harvard Meteorological Studies, No. 6. Cambridge, MA: Harvard University Press, 1943.

[20] Goody RM. A statistical model for water-vapor absorption. Q J of the Roy Met Soc 1952;78:165–9.

[21] Harmann JM, Perrin MY, Ma Q, Tipping RH. The infrared continuum of pure water vapor: calculations and high-temperature measurements. J Quant Spectrosc Radiat Transfer 1993;49:675–91.

[22] Modak AT. Exponential wide band parameters for the pure rotational band of water vapor. J Quant Spectrosc Radiat Transfer 1979;21:131–42.

[23] Wang W-C. An analytical expression for the total band absorptance of infrared-radiating gases. J Quant Spectrosc Radiat Transfer 1983;29:279–81.

[24] Felske JD, Tien CL. A theoretical closed-form expression for the total band absorptance of infrared gases. International Journal of Heat and Mass Transfer 1974;17:155–8.